Interfacial finger cells in a system coupling steady Soret-driven convection and solidification

X. Jin and L. Hadji
Department of Mathematics, The University of Alabama, Tuscaloosa, Alabama 35487
(Received 2 May 1994)

An analysis is conducted on the coupling between thermosolutal convection due to the Soret effect and a solid-liquid interface. This phase boundary forms when a thin layer of a dilute binary mixture is partially solidified from above. A nonlinear evolution equation for the amplitude of the concentration perturbation has been derived [L. Hadji, Phys. Rev. E **47**, 1078 (1993)]. The derivation takes into account the coupled effects of steady convection in the Soret regime and the deformations in the solid-liquid interface. In this paper, the solution of the equation is reexamined using a fully implicit finite difference scheme combined with Newton linearization with coupling. We have obtained results which were previously unobtainable when a fully explicit scheme was used. It is found that, for a range of values of the various parameters, the solid-liquid interface exhibits a cellular morphology consisting of thin fingers that extend deep into the liquid.

PACS number(s): 47.27.Te, 68.45.−v, 64.70.Dv, 81.10.Fq

I. INTRODUCTION

For the purpose of analyzing the coupling between nonlinear convection due to the Soret effect and solidification, Hadji [1] considers the freezing from above of a thin layer of a dilute binary mixture that is confined between two horizontal, rigid, perfectly heat conducting and impermeable plates. The temperature difference between the plates is selected so as to allow for the partial solidification of the mixture. The stationary solid-liquid interface, across which coexist a solid and a liquid phase, is assumed to be planar in the absence of fluid flow, and deformable by the action of convection currents. It is also assumed that the thermal diffusion coefficient in the liquid phase resulting from the Soret effect is independent of concentration so that the equations describing the preconvective state are all linear in the vertical coordinate. Furthermore, changes in the concentration that are associated with the solute rejection or incorporation at the interface, as well as changes in the thermophysical properties of the fluid upon freezing, are neglected. These assumptions were necessary for the nonlinear analysis of the coupling between Soret-driven convection and interface deformations to be tractable.

The governing system of equations consists of the conservation equations for mass, momentum, heat, and solute in the Boussinesq approximation. Only heat conduction is considered in the solid phase. These equations are nondimensionalized using the depth of the liquid layer in the motionless state for the length scale and the thermal diffusion time for the time scale. The concentration is scaled by the Soret-induced concentration gradient existing between the planar interface and the lower plate. In the limit of infinite Prandtl number and large positive separation ratio S, the convective state can be described by the following evolution equation [1,2]:

$$\frac{\partial f}{\partial t} = -f_{xxxx} - 2f_{xx} - \beta f - a f_x f_{xxx} + [(f_x)^3]_x - \tau a (f_x f_{xx})_x + 15a (f f_{xx})_{xx} + b (f_x)^2 - 15b (f^2)_{xx} , \tag{1}$$

where $f(x,t)$ represents the leading order concentration and where the coefficients a and b are complicated functions of the independent physical parameters of the problem, namely the solid layer thickness A, the Lewis number τ, and the dimensionless liquidus slope δ,

$$a = \frac{A}{2(1+A)} \left[\frac{7}{3\chi} \right]^{1/2}, \quad b = \frac{7\chi\zeta'}{30^{3/2}}, \quad \zeta = \frac{10^{3/4}\zeta'}{7^{1/4}\chi^{3/4}\tau} . \tag{2a}$$

The expression for χ is given by

$$\chi = \frac{17}{462} + \frac{25(1+S)\tau}{231S} - \frac{(1+S)(1+2A)\tau}{4S(1+A)} . \tag{2b}$$

As noted in Hadji [1], the evolution equation, Eq. (1), is mathematically well posed only for the range of parameters A, S, and τ, which satisfy $\chi > 0$. We have also adopted the scaling $\delta = -\epsilon^2\zeta'$, where ζ' is an order-one quantity, for the nondimensional liquidus slope in order to couple the leading orders of interface deformations and convective perturbations. When the mixture is in convective motion, the interface is located at $z = 1 + \epsilon^2\eta_2$, where

$$\eta_2 = \frac{-\tau A}{2(1+A)} \frac{\partial^2 f}{\partial x^2} + \zeta' f . \tag{2c}$$

II. ANALYSIS OF THE EVOLUTION EQUATION

A linear stability analysis of Eq. (1) reveals that the trivial solution is stable for $\beta > 1$, but loses stability to a

cellular state with wave number equal to 1 when the scaled Biot number is less than 1. For the purpose of analyzing the bifurcation that occurs at $\beta=1$, we consider an asymptotic study around the zero solution in the vicinity of the bifurcation point $\beta=1$. Following a standard approach, we substitute the following expansions in Eq. (1):

$$\beta=1-\gamma\beta_1-\gamma^2\beta_2+\cdots ,$$

$$f=\gamma f_1+\gamma^2 f_2+\gamma^3 f_3+\cdots , \quad \frac{\partial}{\partial t}=\gamma^2\frac{\partial}{\partial s} ,$$

where the perturbation parameter satisfies $0<\gamma\ll 1$.

The resulting sequence of problems is solved at each order. The leading order problem yields

$$f_1(x,s)=p(s)\cos(x) , \tag{3a}$$

and at the next order in γ the removal of secular terms yields $\beta_1=0$ and

$$f_2(x,s)=p^2[a(2\tau-59)/2+b+a(30-\tau)] +(p^2/18)[59b-(2\tau-59)a] . \tag{3b}$$

Finally, to the cubic approximation in γ we obtain the sought Landau equation for the evolution of the amplitude $p(s)$,

$$\frac{dp}{ds}=\beta_2 p+lp^3 , \tag{4a}$$

where the Landau constant l depends in a complicated fashion on the parameters of the problem, and is given by

$$l=-[a(a\tau)^2+\tau(52a^2-50ab)-2546b^2-7831ab -5285a^2+27]/36 . \tag{4b}$$

A negative l corresponds to supercritical stability with equilibration, while a positive constant implies a finite amplitude instability. One notes from Eq. (4b) that l is negative for $b=0$ and $a=0$, and positive for large enough values of b or a. We also note, from Eq. (2a), that the nonvanishing of the coefficients b and a is due to the nonvanishing of the parameter ζ and to the asymmetry in the boundary conditions due to the solid layer formation [see Eq. (2.11b) in Ref. [1]]. Consequently, the emergence of the subcritical instability is caused by the coupling between temperature, concentration, and interfacial deformations at the solid-liquid interface. Figure 1 depicts the boundaries in the parameter space of the problem, separating supercritical and subcritical bifurcations from the planar state. These boundaries depend on four physical parameters: the separation ratio S, the Lewis number τ, the solid thickness A, and the scaled liquidus slope ζ. We have fixed two pairs of values for S and τ satisfying the well-posedeness condition Eq. (2b). The first pair is $S=0.035$ and $\tau=10^{-5}$, and the second pair is $S=0.035$ and $\tau=10^{-3}$. The transition boundaries are then obtained by solving for ζ as a function of A for the roots of the function $l=0$. The numerical task of determining the roots is accomplished by using the bisection method.

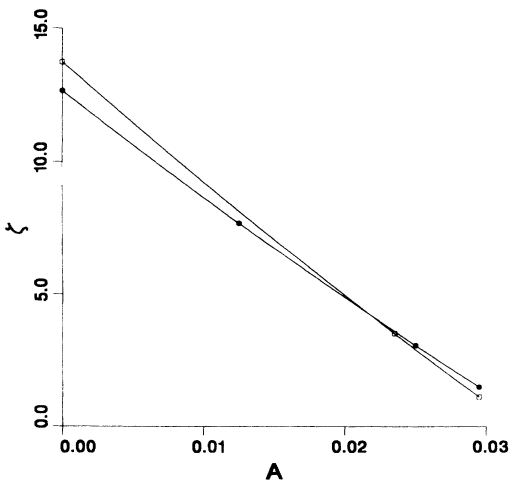

FIG. 1. Plot of the region of subcriticality (above the curve) as determined from Eq. (4b) for $S=0.035$, $\tau=10^{-5}$ (●), and $\tau=10^{-3}$ (□).

III. NUMERICAL RESULTS

We consider the numerical solution of Eq. (1) in a periodic box of length 8π. We have adopted a finite difference scheme that is fully implicit. We have used forward Euler differencing for the time derivative term, and a second-order central difference representation for the spatial derivatives that are evaluated at time step $(n+1)$. The nonlinear terms are linearized by making use of Newton linearization with coupling [3]. This method yields a truncation error $O(\Delta t,\Delta x^2)+O(\Delta t^2)/O(\Delta x)$; consequently, mesh size must be chosen such that $(\Delta t^2)/(\Delta x)$ remains small for both stability and consistency of the scheme. This method allows the solution of Eq. (1) for parameter values that were inaccessible when a fully explicit scheme was used. The latter method requires the time step, as determined from a linear stability analysis, to be highly constrained; even for small time step, numerical instabilities developed for large values of ζ.

We have investigated numerically the evolution of the initial condition $0.1\cos(x)$ for a range of parameter values associated with the subcritical region that was determined theoretically (see Fig. 1). We fixed the values for S, τ, and A to be 0.035, 0.001, and 0.1, respectively, and then we investigated the evolution of the initial profile $0.1\cos(x)$ for several values of $\beta>1$. Figure 2 shows a run with $\beta=1.4$ and two values of ζ. We note that for $\zeta=0$ the initial condition evolves toward the trivial solution, while for $\zeta=400$ a nontrivial cellular state has developed. These findings are in qualitative agreement with the theoretical results. For the parameter values that we have considered, our theory, Fig. 1, predicts finite amplitude solutions for $\zeta\geq 10$. However, in our numerical simulations, we had to take ζ as large as 400 before nontrivial solutions were found.

We have also considered the influence of the undercooling effects, represented by the parameter ζ, on the convective cells. Figure 3 shows the development of the initial profile into steady states for ζ values ranging be-

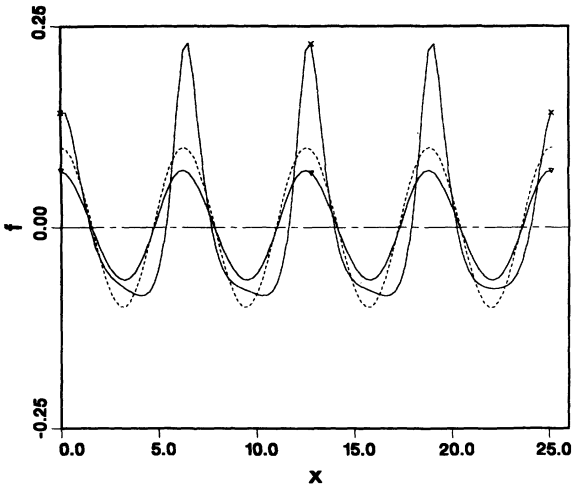

FIG. 2. Plot showing the time development of the initial condition (— — —) for parameter values: $S=0.035$, $\tau=0.001$, $A=0.10$, and $\beta=1.4$ for $\zeta=0.0$ (∇) and $\zeta=400$ ($\times$).

tween 0 and 400. We notice that increases in ζ lead to regions with $f \geq 0$ narrower than those with $f \leq 0$, and to an increase in the amplitude. In the narrow regions, the cells are long, thin, and have sharp peaks, while in the wider regions the cells have rounded tips for $100 \leq \zeta \leq 200$. This is due to the fact that in regions where $f<0$, both the liquid height and the temperature difference are smaller than those required for convection onset, while the opposite scenario holds where $f>0$. Therefore, regions where $f>0$ are relatively more unstable than regions where $f<0$. The convection currents that initiate in the unstable regions penetrate the neighboring stable regions, thus leading to a periodic array of wider cells that are lean in solute, separated by narrow and tall solute rich cells. Since the shape of the interface conforms to the convection pattern in the fluid, the interface will then consist of wide cells with rounded tips separated by narrow cells with sharp tips [see Fig. 4(a)].

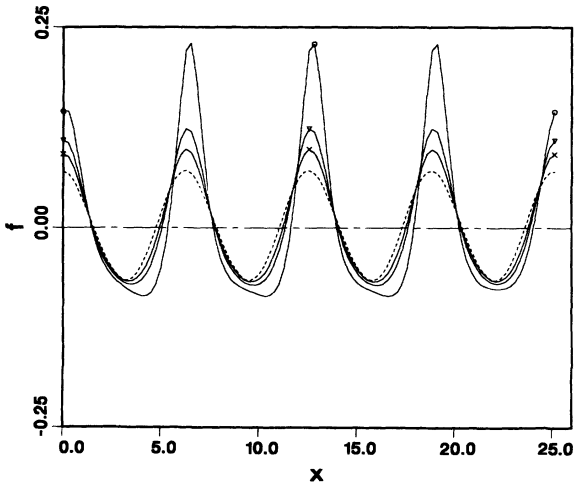

FIG. 3. Plot of the steady state solutions of Eq. (1) for $S=0.035$, $\tau=0.001$, $A=0.1$, $\beta=1.4$, and $\zeta=0$ (— — —), 300 ($\times$), 400 (∇), 500 ($\circ$).

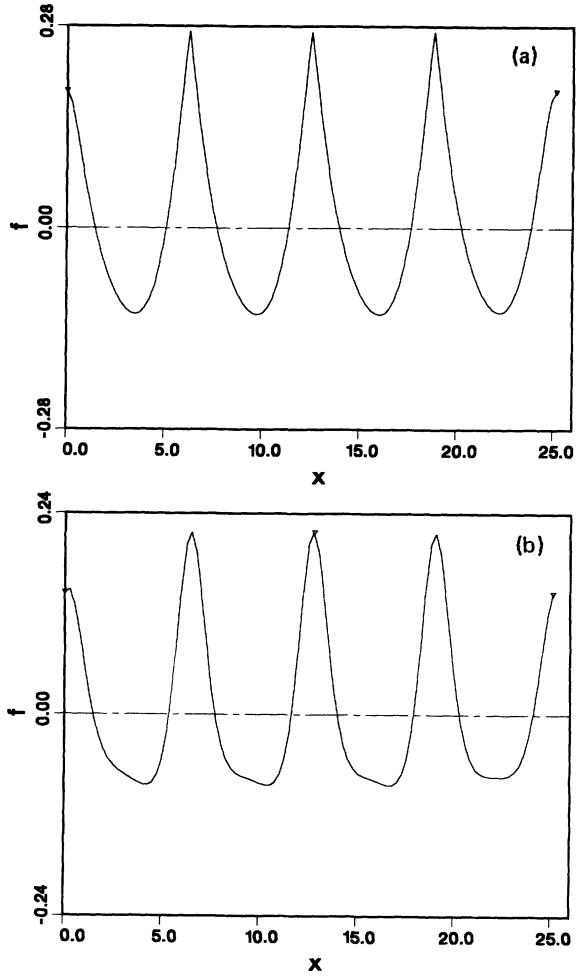

FIG. 4. Steady state solutions to Eq. (1) for $S=0.035$, $\tau=0.001$, $A=0.1$, $\beta=1.4$, and $\zeta=200$ (a), $\zeta=400$ (b).

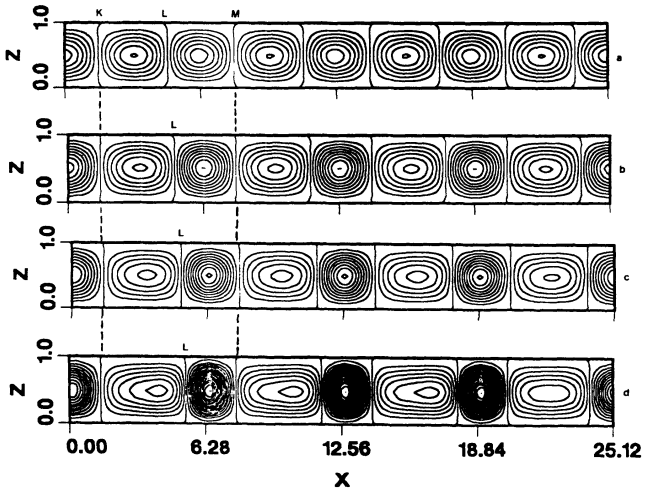

FIG. 5. Plots of the cell pattern for parameter values $S=0.035$, $\tau=0.001$, $A=0.1$, and $\beta=1.4$ and for $\zeta=0$ (a), 300 (b), 400 (c), and 500 (d). The location of the streamline denoted by the letter L is 4.71 in (a), 4.77 in (b), 5.026 in (c), and 5.2778 in (d). The values of ψ of maximum absolute values in the left and right cell, respectively, are $-0.000\,122\,6$ and $0.000\,123\,4$ in (a), $-0.000\,124\,9$ and $0.000\,182\,5$ in (b), $-0.000\,122\,3$ and $0.000\,230\,6$ in (c), and $-0.000\,156\,1$ and $0.000\,431\,0$ in (d).

When ζ exceeds the value of about 300, a tilting in the cells also develops in the wider regions as shown in Fig. 4(b). The size of these cells, as predicted by the dispersion formula, equals 2π [1]. This trend seems to be going toward the thin interfacial fingers, which have been observed experimentally. The experimental results of Jackson [4] reveal an interfacial structure in which the thin fingers of solute extend into the melt associated with a tilting of the cells during the directional solidification of tetrabromomethane, CBr_4. These results pertain to an interface that becomes morphologically unstable at some pulling rate, with the cells's size $\sim 30\mu$.

These effects are more apparent in the plot of the steamlines, which at the leading order in ϵ are given by [1]

$$\psi(x,z)=30\tau(z^4-2z^3+z^2)f \ . \tag{5}$$

The cell pattern that is shown in Fig. 5 corresponds to values of ζ ranging from 0 to 400. We follow the evolution of the cell pattern with increasing ζ in the box of length 2π located between the two streamlines $x=\pi/2$ and $x=5\pi/2$ denoted by the letters K and M, respectively, in the figure. When $\zeta=0$, there are two counterrotating cells symmetric about $z=0.5$ and the line $x=3\pi/2$, denoted by the letter L in the figure. As ζ is increased by intervals of 100, the left cell ($\psi<0$) becomes wider and the right cell ($\psi>0$) narrower. The thin cells are regions of higher velocity than the wider cells. In the wider cells, the center of the cell migrates to the right with increasing values of ζ, the center of the cell being a point of maximum velocity.

ACKNOWLEDGMENTS

This work has been supported by a grant from the School of Mines and Energy Development (SOMED), and with computing resources from the Alabama Supercomputer Network's Cray X/MP-24 supercomputer.

[1] L. Hadji, Phys. Rev. E **47**, 1078 (1993).

[2] L. Hadji, X. Jin, and W. Schreiber, in *Developments in Theoretical and Applied Mechanics,* edited by I. C. Jong and F. A. Akl (University of Arkansas Press, Fayetteville, AR, 1994), Vol. XVII, pp. 474–483.

[3] D. A. Anderson, J. C. Tannehill, and R. H. Pletcher, *Computational Fluid Mechanics and Heat Transfer* (Hemisphere, New York, 1984).

[4] K. A. Jackson, in *Solidification,* edited by T. J. Hughel and G. F. Bolling (American Society for Metals, Metals Park, OH, 1971), p. 133.